

Quantum chemical approach to atomic manipulation of chlorobenzene on the Si(111)-7 × 7 surface: Resonance localization, vibrational activation, and surface dynamics

M. Utecht,¹ R. E. Palmer,² and T. Klamroth^{1,*}

¹*Institut für Chemie, Universität Potsdam, Karl-Liebknecht-Strasse 24-25, D-14476 Potsdam-Golm, Germany*

²*College of Engineering, Swansea University, Bay Campus, Fabian Way, Swansea SA1 8EN, United Kingdom*

(Received 28 April 2017; published 12 July 2017)

We present a cluster model to describe the localization of hot charge carriers on the Si(111)-7 × 7 surface, which leads to (nonlocal) desorption of chlorobenzene molecules in scanning tunneling microscope (STM) manipulation experiments. The localized charge carriers are modeled by a small cluster. By means of quantum chemical calculations, this cluster model explains many experimental findings from STM manipulation. We show that the negative charge is mainly localized in the surface, while the positive one also resides on the molecule. Both resonances boost desorption: In the negative resonance the adatom is elevated; in the positive one the chemisorption bond between the silicon surface adatom and chlorobenzene is broken. We find normal modes promoting desorption matching experimental low-temperature activation energies for electron- and hole-induced desorption.

DOI: [10.1103/PhysRevMaterials.1.026001](https://doi.org/10.1103/PhysRevMaterials.1.026001)

Manipulations of single molecules or atoms with the scanning tunneling microscope (STM) [1–9] are not only important for nanotechnology in general and information technology in particular. They also offer well-controlled model systems for reactions at surfaces or interfaces induced by charge carriers with low energies on the order of a few eV. Such reactions, like the breaking of DNA strands [10] or photocatalytic water splitting [11], are relevant for a broad range of fields. Therefore, a number of elementary reaction steps—for instance, dissociation [12], desorption [13], and bond formation [14]—have been studied with and induced by STM.

One of these model system is chlorobenzene on Si(111)-7 × 7, which has been subject to intensive studies like similar systems—for instance, benzene or toluene—on the same surface. Desorption [15] of chlorobenzene from a Si(111)-7 × 7 surface can be induced in a one-electron (positive surface bias voltage) or a one-hole process (negative bias voltage) and is to a large extent nonlocal [13,16]. Also, dissociation of the carbon-chlorine bond has been reported in either a two-electron process [17] or a thermally assisted one-electron process [18]. The theoretical modeling of STM manipulations often relies on the description of so-called inelastic electron tunneling and is therefore local in nature. For such modeling one either couples the tunneling electrons to permanent dipole moments of the adsorbate [19], or transient occupation of negative or positive ion resonances [20] is assumed, in either the below- [19–22] or the above-threshold limit [23–25]. Such models often rely on a few representative potential energy surfaces for the relevant states, similar to models well established in surface photochemistry [26,27].

In this paper we report cluster calculations aiming at the characterization of the negative and positive ion resonances involved in the nonlocal STM-induced desorption of chlorobenzene from Si(111)-7 × 7. These investigations are driven by recent experimental findings [2,4,28–30]. Here we focus on (i) the geometric changes and charge localizations

in the relevant resonances driving the nonlocal desorption at negative and positive bias voltages and (ii) the origin of the measured low-temperature thermal activation energies. In the most recent experimental works the nonlocal desorption from Si(111)-7 × 7 was investigated for toluene (driven by holes) [2] and for chlorobenzene, toluene, and benzene (driven by electrons) [4]. It was shown that the distance and temperature dependence of electron-driven desorption can be described by a model of hot surface-charge diffusion. The threshold voltage for this process was determined as 1.4 V. The hole-driven desorption could also be successfully modeled by a diffusion process, which succeeds an initial period of coherent charge expansion, i.e., ballistic hole transport near the injection site (<15 nm), which leads to smaller reaction probabilities. For holes, a threshold surface bias of –1.2 V was reported. In Ref. [28] it was shown that the hole-driven desorption of toluene from Si(111)-7 × 7 is closely related to the excitation of the surface silicon adatom for positive bias voltage. For the thermally activated one-electron-driven process in Ref. [29], a low-temperature activation energy of (21 ± 4) meV was determined for chlorobenzene. Recently, a refined analysis gave an activation energy of (13 ± 3) meV for electrons, while new experiments gave a low-temperature thermal activation energy of (60 ± 10) meV for holes [30], also for chlorobenzene. Up to this point in time the origin of these vibrational enhancements has been unclear. In this paper, we present calculations, which show the charge localizations and geometrical changes in the resonance states and explain the low-temperature thermal activation energies for desorption as well as the connection of the hole-driven desorption to the surface silicon adatom excitation.

In Ref. [32] we applied cluster models to chlorobenzene on Si(111)-7 × 7 in order to calculate the electronic structure of chemi- and physisorbed chlorobenzene, which forms a foundation for the current work. Cluster models also have been successfully applied to other STM-manipulations of hydrocarbons on silicon surfaces, for instance benzene on Si(100) [23] or cyclooctadien on Si(100)[21]. For chlorobenzene on Si(111)-7 × 7 we computed a value—at that time unexpected—of ≈1.6 eV for the chemisorption energy at

*klamroth@uni-potsdam.de

the B3LYP [33] level of theory together with Grimmes D3 dispersion correction [34]. In Ref. [35] a value of 1.0 eV was reported based on thermal desorption spectra. Recent time-lapse STM experiments [36] found, however, that the formerly used preexponential factor was too small and determined a revised chemisorption energy of ≈ 1.4 eV, in good agreement with our calculations. In these calculations a rather large cluster was used with 67 silicon atoms of the faulted half of the unit cell. We will use this cluster as a reference here (termed “large cluster” in the following). In Ref. [32] all degrees of freedom of the large cluster were relaxed. Here, we fix the coordinates of the saturating hydrogen atoms as done for the small cluster (see below).

We use a smaller cluster to simulate localized hot charge carriers. We start from a centrosymmetric unit cell reported in Ref. [31], based on a density functional theory slab calculation of the so-called dimer-atom-stacking fault structure [37]. We use the two top double layers of the faulted half of the unit cell shown in Fig. 1(a). This half contains nine so-called adatoms (Si_a) and three rest atoms (Si_r). The lines show the cuts made to obtain the small cluster containing a center adatom, one rest atom, and all silicon atoms with maximal “two bonds distance” to these. All Si-Si bonds cut were saturated with hydrogen atoms, which were fixed such that the resulting H-Si bond points in the same direction as the broken Si-Si bond with a Si-H bond length of 1.51 Å. Apart from the fixed Cartesian coordinates of the hydrogen atoms, all other degrees of freedom were fully optimized if not stated otherwise. In this way, we obtain a small cluster having 21 silicon atoms saturated by 34 hydrogen atoms. With this small cluster, we model localized, hot charge carriers at the surface, simply by setting the charge to +1 or -1 in the quantum chemical calculations. We avoid the calculation of charged excited states of the extended surface by this procedure within our cluster approach. In addition, these excited states would need to be

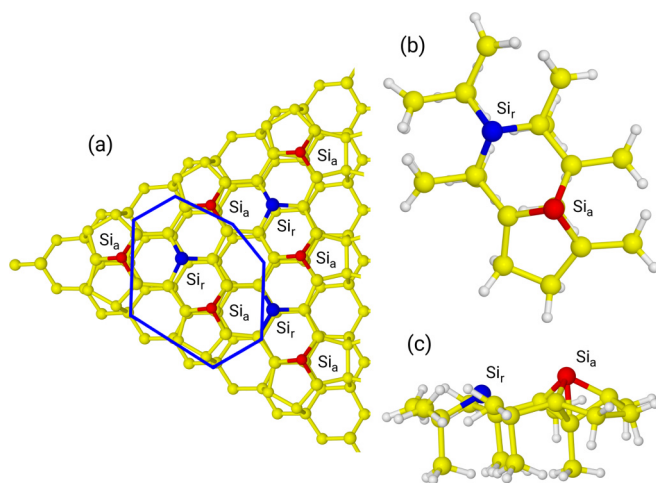


FIG. 1. The two top double layers of the faulted half of the Si(111)- 7×7 surface unit cell taken from Ref. [31] are shown on the left (a). The lines indicate cuts made to obtain the small cluster used, which is shown on the right in top (b) and side (c) views with the saturating hydrogen atoms. Hydrogen atoms are shown in white, rest atoms (Si_r) in blue, adatoms (Si_a) in red, and all other Si atoms in yellow.

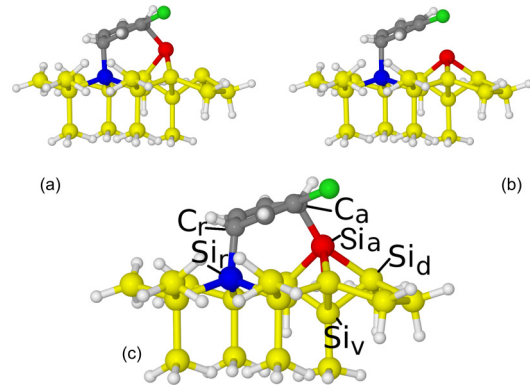


FIG. 2. Optimized chemisorption geometries for the anionic (a), cationic (b), and neutral (c) system. For the neutral system, the labels used for special atoms are given. For the cluster atoms the colors used are the same as in Fig. 1; the chlorine atom of the molecule (in *ortho* position to C_a) is shown in green and the carbon atoms in gray.

in a superposition in order to represent a localized hot charge carrier. We calculate ionization potentials (IPs) and electron affinities (EAs) for the small cluster and the large cluster, which we take as a representation for the extended surface, in order to estimate the excitation energy of the hot charge carriers represented by the charged small cluster. The differences between the IPs and EAs are taken as a rough measure for the energy needed to form the localized resonance, i.e., the hot charge carrier (see below). The requirements for the small cluster, which follow from this procedure, are (i) it should describe the chemisorption in the neutral state correctly and (ii) yield resonance energies in the right range compared with experiment.

We performed all calculations at the B3LYP-D3/6-31G* level of theory as implemented in GAUSSIAN09 [38]. The results of Ref. [32] indicate that a basis set of double- ζ quality is sufficient if counterpoise corrections (CPCs) [39] are applied to adsorption energies. The optimized chemisorption geometries are shown in Fig. 2 for the anionic (a), cationic (b), and neutral (c) systems. In all calculations the most stable structural configuration for the neutral system is used, i.e., the one with the chlorine *ortho* to the carbon atom bound to the silicon adatom (C_a). For the neutral small cluster we get 1.443 eV chemisorption energy compared with 1.639 eV for the large one (both with CPC). Thus, even the small cluster is still capable of describing the electronic structure of the chemisorbed system.

In contrast, for the charged clusters we get large differences between the adsorption energies, 0.088 eV for the anionic small cluster and 0.433 eV for the cationic one, compared with 1.526 and 1.576 eV for the corresponding large clusters (all values with CPC). If one compares the vertical EA and IP for the chemisorbed systems computed by Δ SCF (delta self consistent field), one gets a 1.91-eV higher IP and a 2.18-eV lower EA for the small cluster compared with the large cluster. As stated above, these values represent a rough estimate of the excess energies of localized hot charge carriers, as represented by the charged small cluster, and are within the experimental energy range. As already mentioned, threshold surface bias voltages of 1.4 V (electrons) [4] and -1.2 V (holes) [2] are

TABLE I. Selected bond lengths for chemisorption (C) and selected physisorption (P) minima of the neutral, anionic, and cationic small cluster. All values given in Å. For the labeling of the atoms, see Fig. 2(c).

	$R_{\text{Si}_r\text{-C}_r}$	$R_{\text{Si}_a\text{-C}_a}$	$R_{\text{Si}_a\text{-Si}_d}$	$R_{\text{Si}_a\text{-Si}_v}$
Neutral (C)	2.018	2.034	2.627	2.734
Anion (C)	1.990	2.075	3.024	2.966
Cation (C)	2.109	2.961	2.502	2.545
Neutral (P)	4.120	3.085	2.443	2.442
Anion (P)	4.008	3.768	2.517	2.689
Cation (P)	5.017	2.787	2.434	2.476

found for the resonance-driven desorption, which correspond to minimal excess energies of 1.4 eV for electrons and 1.2 eV for holes.

We calculated the electrostatic potential derived charges (ESP charges) [40,41] for the optimized geometries shown in Fig. 2 in order to clarify where the additional charge is localized. In case of the neutral system, we obtain for the small cluster a net charge transfer from the cluster to the molecule. This is reflected by a sum of ESP charges of -0.213 e on the adsorbate. This is nearly identical to the large cluster, where we find -0.286 e. For the anionic small cluster we find that only -0.063 e of the additional one electron charge is on the adsorbate and the main part of the hot electron is in the surface, to a large extent on the adatom (Si_a) and the Si atom below the adatom (Si_b). In contrast, we find $+0.286$ e of the excess positive charge, i.e., the one hole, on the molecule for the cationic small cluster. As expected, the additional negative and positive charges sit nearly completely in the large cluster (± 0.970 e).

The different charge localizations for the small cluster are nicely reflected by the geometrical changes induced by the localized hot charges, as shown in Fig. 2. Selected bond lengths in the neutral system and charged systems are given in Table I, for both the chemisorbed molecule (C) and the selected physisorption (P) minima. The labeling of the atoms is given in Fig. 2(c). As one can see, the bond from chlorobenzene to the rest atom, $R_{\text{Si}_r\text{-C}_r}$, is not substantially changed by the negative or the positive charge for the chemisorbed systems. In contrast, the bond to the adatom, $R_{\text{Si}_a\text{-C}_a}$, is increased by 0.927 Å in the cationic system, but nearly unchanged in the anion. For the anion the main changes occur in the cluster; specifically, the adatom is lifted out of the surface. This leads to a 0.397 -Å longer bond between the adatom and the atom vertically below, Si_v , and to a 0.232 -Å larger distance to the atom diagonally behind the adatom, Si_d . For the large cluster all changes in the corresponding bond lengths are well below 0.01 Å in magnitude. This also indicates, together with the small changes in the chemisorption energies for the large cluster, that the charge localization in the direction normal to the surface in the large cluster—which is comparable to the one in the small cluster—is of minor importance for the chemisorption. Thus, we conclude that a significant component of the positive hot charge is located on the adsorbate and lifts one end of the molecule directly away from the surface. However, the negative hot charge is mainly localized in the surface and pushes the adsorbate away from the surface through an elevation of the

adatom. This is in agreement with the experimental results in Ref. [28]. There it was shown that the hole-induced desorption is connected to an excitation of the adatom.

In order to characterize the origin of the low-temperature activation energies for nonlocal desorption via electrons, (13 ± 3) meV, and holes, (60 ± 10) meV [30], we performed a normal mode analysis for the neutral small cluster. We artificially set the mass of the fixed hydrogens used for saturation to be 10^{15} amu (1.66×10^{-12} kg) for these calculations. A single excitation of a vibration with a frequency corresponding to a few tens of meV is a very small energy compared with the chemisorption energy in the neutral state, in which the desorption is most likely to occur due to the very short lifetimes of hot charge carriers. Therefore, we assume that the desorption is enhanced by vibrational preexcitation, due to an enhanced probability to form the localized hot charge carrier. A displacement in a suitable normal coordinate towards the resonance geometry should lower the energy difference between the neutral and the resonance states and lead to larger overlaps between vibrational wave functions in both states. In that way, the formation of the localized hot charge carrier can be enhanced. Therefore, the linear transit coordinate between optimized charged systems and the neutral geometry is projected on the normal coordinates, as done in Ref. [42]. The modes with a sizable contribution to the linear transit path in the range of the experimental activation energies are compared with the geometrical changes due to charging discussed in the previous paragraph. Note that a direct identification of the important modes from the magnitude of the projection coefficients is difficult, because (i) the reduced mass of the respective mode enters through the normalization and (ii) the linear transit path here is a large amplitude motion, along which the character of the normal modes might change substantially. By this procedure we were able to identify the two normal modes sketched in Fig. 3. In panel (a), a normal mode at 500.0 cm^{-1} (61.99 meV) is shown, which is basically a molecular mode, but nevertheless contains a large $R_{\text{Si}_a\text{-C}_a}$ elongation. This mode should promote the transition to the localized, hot cation. As a promoting mode for the anion, we find an adatom wagging mode at 96.5 cm^{-1} (11.96 meV), which is displayed in Fig. 3(b). The energies of these modes are remarkably similar to the experimental values. The two vibrations shown here will not be represented by single normal modes on an extended surface; instead they will couple to several phonon modes. For instance, we find substantial contributions of the $\text{Si}_a\text{-C}_a$ stretch in more than ten modes between 490 and 505 cm^{-1} in the large cluster, while the adatom wag is still fairly represented by a single mode at 91.3 cm^{-1} . However, the energetic positions of such localized vibrational resonances should not change significantly in an extended system, because the energy is mainly determined by the strength of the local chemical bonds and the masses of the involved atoms.

Several experimental findings have also been reported for physisorbed chlorobenzene molecules [30,43] and the clean $\text{Si}(111)\text{-}7 \times 7$ surface. Thus, we calculated optimized physisorption geometries for the neutral and charged systems shown in Fig. 4. Note that there are many physisorption minima, all with comparable energies. In Fig. 4, we show the ones geometrically closest to the neutral chemisorption

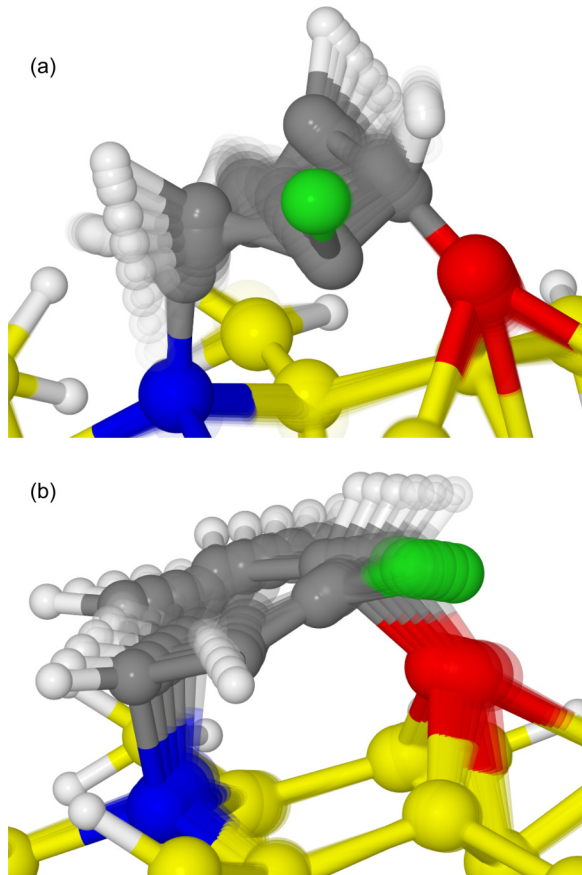


FIG. 3. Sketches of normal modes associated with thermally enhanced desorption in STM manipulation. Shown are overlays with increasing opacity along selected normal coordinates of the small cluster. (a) A mode containing the $\text{Si}_a\text{-C}_a$ stretch at 500.0 cm^{-1} (61.99 meV); (b) a mode containing the silicon adatom wag at 96.5 cm^{-1} (11.96 meV) (for details, see text).

minimum energy configuration. We obtain physisorption energies of 0.497 eV for the neutral system, 0.593 eV for the cation, and 0.316 eV for the anion (all values with CPC). As we get chemisorption energies of 0.088 eV for the anion and 0.433 eV for the cation (see above), this means that physisorption is energetically preferred over chemisorption for the localized charges. The corresponding bond lengths can be found in Table I. One can see that the added positive charge does not influence the physisorption very much. The large changes in $R_{\text{Si}_i\text{-C}_r}$ and $R_{\text{Si}_a\text{-C}_a}$ are mostly due to an in-plane rotation of the adsorbate compared with the chemisorption configuration. For the anion, one again finds an adatom elevation, which pushes part of the chlorobenzene away from the surface [see Fig. 4(a) compared with Figs. 4(b) and 4(c)]. Moreover, we find almost the same adatom elevation in the case of a clean small cluster with no adsorbate: $R_{\text{Si}_a\text{-Si}_i}$ changes by 0.262 \AA (clean) and 0.247 \AA (physisorbed). This fits experimental findings that adatom excitation can only be achieved with positive bias voltages [44], i.e., electron, not hole, injection.

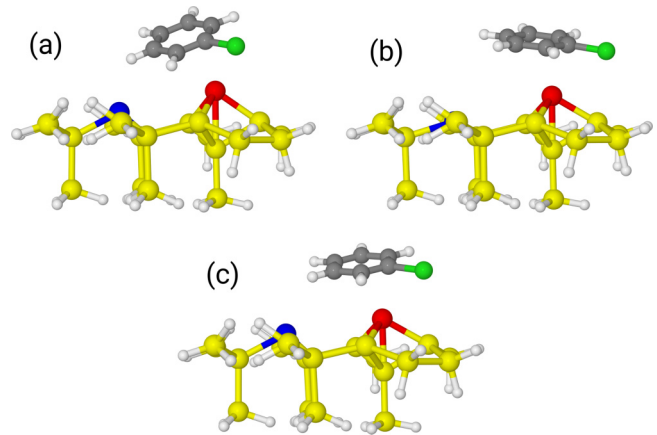


FIG. 4. Selected physisorption minima for the anionic (a), the cationic (b), and the neutral (c) systems. The color code is the same as in Fig. 2.

Finally, we report, as an independent confirmation of the validity of our cluster model, the calculated energy of the transition state between the shown neutral chemisorption and physisorption minima. An energy of 1.05 eV (with CPC) was found relative to the chemisorption minimum in good agreement with the experimental value of $1.19 \pm 0.03\text{ eV}$ [36] obtained from adsorption-site-specific time-lapse STM. This relates to the activation energy for the thermally assisted one-electron dissociation of the carbon-chlorine bond [12].

To summarize, we presented a cluster model which can explain many experimental findings for the nonlocal STM manipulation of chlorobenzene on $\text{Si}(111)\text{-}7 \times 7$. We estimated from calculated IPs and EAs that the energies of the models for hot charge carriers are in the right energy range. Both resonances, the negative and the positive ion, induce geometry changes, which ultimately point towards desorption of the adsorbate. The negative ion is localized in the silicon surface, not on the molecule. Moreover, we find normal modes promoting desorption, with different character for the positive and negative ion resonances, in both cases with energies matching the experimental low-temperature activation energies found in nonlocal desorption measurements. Finally, the cluster model yields chemisorption and physisorption energies in line with experiments, as well as the barrier between chemisorption and physisorption states. The negative ion resonance of the clean cluster promotes adatom excitation, again in agreement with experimental results. All these points indicate that our cluster calculations are able to characterize not only the chemisorption ground state but also the short-lived charged resonances. As a next step and further test, we plan to build on this cluster model approach and to develop an open quantum system dynamics model for this system.

T.K. and M.U. acknowledge financial support from the Deutsche Forschungsgemeinschaft through Grant No. KL-1387/3-1. R.E.P. acknowledges financial support from the EPSRC and many enjoyable discussions with Scott Holmes.

[1] J. Repp, W. Steurer, I. Scivetti, M. Persson, L. Gross, and G. Meyer, *Phys. Rev. Lett.* **117**, 146102 (2016).

[2] K. R. Rusimova, N. Bannister, P. Harrison, D. Lock, S. Crampin, R. E. Palmer, and P. A. Sloan, *Nat. Commun.* **7**, 12839 (2016).

- [3] K. Huang, L. Leung, T. Lim, Z. Ning, and J. C. Polanyi, *ACS Nano* **8**, 12468 (2014).
- [4] D. Lock, K. R. Rusimova, T. L. Pan, R. E. Palmer, and P. A. Sloan, *Nat. Commun.* **6**, 8365 (2015).
- [5] C. Nacci, A. Viertel, S. Hecht, and L. Grill, *Angew. Chem., Int. Ed.* **55**, 13724 (2016).
- [6] J. A. Strosio and D. M. Eigler, *Science* **254**, 1319 (1991).
- [7] I.-W. Lyo and P. Avouris, *Science* **253**, 173 (1991).
- [8] L. Bartels, G. Meyer, and K.-H. Rieder, *Phys. Rev. Lett.* **79**, 697 (1997).
- [9] W. Ho, *J. Chem. Phys.* **117**, 11033 (2002).
- [10] B. Boudaïffa, P. Cloutier, D. Hunting, M. A. Huels, and L. Sanche, *Science* **287**, 1658 (2000).
- [11] K. Maeda and K. Domen, *J. Phys. Chem. Lett.* **1**, 2655 (2010).
- [12] S. Sakulsermsuk, P. A. Sloan, and R. E. Palmer, *ACS Nano* **4**, 7344 (2010).
- [13] P. A. Sloan, S. Sakulsermsuk, and R. E. Palmer, *Phys. Rev. Lett.* **105**, 048301 (2010).
- [14] J. R. Hahn and W. Ho, *Phys. Rev. Lett.* **87**, 166102 (2001).
- [15] P. A. Sloan, M. F. G. Hedouin, R. E. Palmer, and M. Persson, *Phys. Rev. Lett.* **91**, 118301 (2003).
- [16] T. L. Pan, P. A. Sloan, and R. E. Palmer, *Chem. Rec.* **14**, 841 (2014).
- [17] P. A. Sloan and R. E. Palmer, *Nature (London)* **434**, 367 (2005).
- [18] P. H. Lu, J. C. Polanyi, and D. Rogers, *J. Chem. Phys.* **111**, 9905 (1999).
- [19] B. N. J. Persson and J. E. Demuth, *Solid State Commun.* **57**, 769 (1986).
- [20] B. N. J. Persson and A. Baratoff, *Phys. Rev. Lett.* **59**, 339 (1987).
- [21] C. Nacci, S. Fölsch, K. Zenichowski, J. Dokić, T. Klamroth, and P. Saalfrank, *Nano Lett.* **9**, 2996 (2009).
- [22] K. Zenichowski, J. Dokić, T. Klamroth, and P. Saalfrank, *J. Chem. Phys.* **136**, 094705 (2012).
- [23] S. Alavi, R. Rousseau, S. N. Patitsas, G. P. Lopinski, R. A. Wolkow, and T. Seideman, *Phys. Rev. Lett.* **85**, 5372 (2000).
- [24] A. Abe, K. Yamashita, and P. Saalfrank, *Phys. Rev. B* **67**, 235411 (2003).
- [25] K. Zenichowski, C. Nacci, S. Fölsch, J. Dokić, T. Klamroth, and K. Saalfrank, *J. Phys.: Condens. Matter* **24**, 394009 (2012).
- [26] P. Avouris and R. E. Walkup, *Annu. Rev. Phys. Chem.* **40**, 173 (1989).
- [27] J. A. Misewich, T. F. Heinz, and D. M. Newns, *Phys. Rev. Lett.* **68**, 3737 (1992).
- [28] K. R. Rusimova and P. A. Sloan, *Nanotechnology* **28**, 054002 (2017).
- [29] T. L. Pan, P. A. Sloan, and R. E. Palmer, *J. Phys. Chem. Lett.* **5**, 3551 (2014).
- [30] S. A. Holmes, Ph.D. thesis submitted to The University of Birmingham, 2017.
- [31] J. Ciston, A. Subramanian, I. K. Robinson, and L. D. Marks, *Phys. Rev. B* **79**, 193302 (2009).
- [32] M. Utecht, T. Pan, T. Klamroth, and R. E. Palmer, *J. Phys. Chem. A* **118**, 6699 (2014).
- [33] A. D. Becke, *J. Chem. Phys.* **98**, 5648 (1993).
- [34] S. Grimme, J. Antony, S. Ehrlich, and H. Krieg, *J. Chem. Phys.* **132**, 154104 (2010).
- [35] Y. Cao, J. F. Deng, and G. Q. Xu, *J. Chem. Phys.* **112**, 4759 (2000).
- [36] D. Lock, S. Sakulsermsuk, R. E. Palmer, and P. A. Sloan, *J. Phys.: Condens. Matter* **27**, 054003 (2015).
- [37] K. Takayanagi, Y. Tanishiro, M. Takahashi, and S. Takahashi, *J. Vac. Sci. Technol., A* **3**, 1502 (1985).
- [38] M. J. Frisch, G. W. Trucks, H. B. Schlegel *et al.*, GAUSSIAN09, Revision D.1, Gaussian Inc., Wallingford, CT, 2009.
- [39] S. F. Boys and F. Bernardi, *Mol. Phys.* **19**, 553 (1970).
- [40] B. H. Besler, K. M. M., Jr., and P. A. Kollman, *J. Comp. Chem.* **11**, 431 (1990).
- [41] U. C. Singh and P. A. Kollman, *J. Comp. Chem* **5**, 129 (1984).
- [42] T. Klamroth, *J. Chem. Phys.* **124**, 144310 (2006).
- [43] X. Lu, J. C. Polanyi, and J. S. Y. Yang, *Nano Lett.* **6**, 809 (2006).
- [44] B. C. Stipe, M. A. Rezaei, and W. Ho, *Phys. Rev. Lett.* **79**, 4397 (1997).